

Latching Control Strategies for a Heaving Buoy Wave Energy Generator in a Random Sea

F Saupe, J C Gilloteaux, P Bozonnet, Y Creff, P Tona

▶ To cite this version:

F Saupe, J C Gilloteaux, P Bozonnet, Y Creff, P Tona. Latching Control Strategies for a Heaving Buoy Wave Energy Generator in a Random Sea. 19th World Congress of the International Federation of Automatic Control, Aug 2014, Cape Town, South Africa. pp.7710 - 7716, 10.3182/20140824-6-ZA-1003.00440. hal-01443922

HAL Id: hal-01443922 https://ifp.hal.science/hal-01443922

Submitted on 23 Jan 2017

HAL is a multi-disciplinary open access archive for the deposit and dissemination of scientific research documents, whether they are published or not. The documents may come from teaching and research institutions in France or abroad, or from public or private research centers.

L'archive ouverte pluridisciplinaire **HAL**, est destinée au dépôt et à la diffusion de documents scientifiques de niveau recherche, publiés ou non, émanant des établissements d'enseignement et de recherche français ou étrangers, des laboratoires publics ou privés.

Latching Control Strategies for a Heaving Buoy Wave Energy Generator in a Random Sea

F. Saupe, J.-C. Gilloteaux, P. Bozonnet, Y. Creff, P. Tona*

* IFP Energies nouvelles, Rond-point de l'échangeur de Solaize, BP 3, 69360 Solaize, France (e-mail: paolino.tona@ifpen.fr).

Abstract: This paper addresses the latching control of wave energy converters. The principle of this control approach is to bring the wave energy generator into resonance with the incident wave using a clamping mechanism. Maximum energy extraction is the control objective. The main challenge in any latching control scheme is to calculate the precise time when to release the device after it has been locked at zero velocity. At the example of a generic heaving buoy device and using real wave data, three latching strategies are compared to a PI velocity control. The simplest considered latching strategy releases the device as soon as the wave force reaches a certain threshold. The other strategies use a short-term wave prediction in order to calculate the latching timing. Imperfect wave predictions based on AR models and imperfect mechanical to electrical and electrical to mechanical power conversions are taken into account. While the imperfect wave predictions impact the achievable performance with the predictive latching strategies, the imperfect power conversions have a high impact on the PI velocity control due to its reactive power flow.

1. INTRODUCTION

The control of wave energy converters via a discontinuous control law, commonly referred to as latching, is addressed in this paper. The principle of latching control is to bring the wave energy generator into resonance with the incident wave by using a clamping mechanism. It is ensured that the latching control needs to draw no significant amounts of power from the net by only activating the clamping mechanism if the velocity of the device is zero. The main aspect of any latching control scheme is the calculation of the precise time to unlatch the device. The optimal timing depends on the incident wave. In a regular sea with monochromatic waves, the problem of determining the optimal timing is easily solved, see e.g. Babarit and Clément (2006). However, in a more realistic irregular sea, the same problem is much harder to solve and has been an active field of research for decades, see Budal et al. (1982); Babarit and Clément (2006); Babarit et al. (2004); Falcão (2008).

Several approaches to latching control in an irregular sea are considered. The first is a simple but effective threshold unlatching which releases the device if the incident wave force reaches a certain threshold, Falcão (2008). The second latching scheme uses a prediction of the incident wave force to calculate a latching timing which is optimal on the considered prediction horizon. The calculations are performed using the full WEC model, Babarit et al. (2003, 2004). In a novel approach, proposed in this paper, the time to unlatch the device is also determined based on a short-term prediction of the incident wave. It is simpler than the approach from Babarit et al. (2003, 2004) as the available horizon of the wave force prediction is only searched for the time interval with the highest

mean up/down force. An eigenvalue analysis of the wave energy generator is sufficient to determine the length of the interval.

Proportional integral (PI) velocity feedback is considered as a reference control. This approach is simple to apply effectively in irregular waves and thus popular in the industry, see e. g. Hansen and Kramer (2011). The downside of a PI velocity control is its reactive power flow, i. e. the fact that power is also taken from the net. The different control strategies are presented in Section 3.

In the literature on short-term wave prediction, algorithms based on auto regressive (AR) models have been established as the state of the art, see e.g. Fusco and Ringwood (2010b,a); Schoen et al. (2011). Accordingly, the robustness of the latching schemes which use a prediction of the incident wave force is analysed by replacing perfect predictions with more realistic predictions based on AR models. Section 4 gives a description of the applied wave prediction algorithm.

The performances of the considered control schemes are benchmarked based on a scenario using wave data recorded at Galway Bay by the Irish Marine Institute. Section 2 presents a generic model of a heaving buoy wave energy generator which is used for the simulations. Imperfect mechanical to electrical and electrical to mechanical power conversion efficiencies are taken into account. Since this effect makes the power which is taken from the net more expensive compared to the produced power, these efficiencies have a great impact on the achievable performance with the PI velocity control and accordingly, the advantages of latching show off nicely. The results of the simulation study are presented in Section 5.

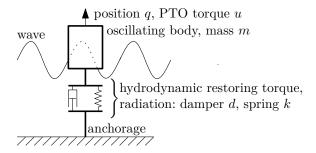


Fig. 1. Simplified model of a wave energy generator.

2. MODELLING APPROACH

This section introduces the mathematical model of a generic heaving buoy point absorber wave energy converter and gives a short characterisation of the considered sea state.

2.1 Model of a Generic Wave Energy Converter

A wave energy converter of the heaving buoy type is considered. The incident wave excites oscillations of the buoy. The installed power take off device (PTO) is used to convert the kinetic energy of the device into useful electric energy. The buoy and the wave interact via the hydrodynamic restoring force (modelled as a spring), a simple radiation force (modelled as a damper) and a constant added mass. The system is depicted schematically in Figure 1. This simple modeling approach is chosen over an approach which takes into account dynamic radiation forces because it allows to change the important system characteristics in an uncomplicated way. Being able to take into account systems with different resonance frequencies allows to establish interesting insights into the suitability of the considered control approaches. It is pointed out that all considered control approaches are also applicable (without modification) to the more general case of a system with a dynamic radiation force and a dynamic added mass term.

With the position q of the oscillating body, the eigenfrequency ω_0 , the damping ζ , the incident wave force w and the PTO force u, the equations of motion of the wave energy converter model are

$$\ddot{q} + 2\zeta\omega_0\dot{q} + \omega_0^2 q = w + u. \tag{1}$$

The relation between the physical parameters mass (including the added mass) m, damping coefficient d, stiffness coefficient k and the parameters parameterising the equations of motion ω_0 , ζ are

$$\omega_0 = \sqrt{\frac{k}{m}}, \ \zeta = \frac{d}{2\omega_0 m}.$$
 (2)

Two example systems are considered in this study. Both have a damping of $\zeta=0.1$ but differ in their eigenfrequencies which lie at $\omega_0=0.22\,\mathrm{Hz}$ and $\omega_0=0.33\,\mathrm{Hz}$.

The instantaneous power output P_i of the device is modelled as a nonlinear function involving the product of the PTO force u and the velocity \dot{q} and an efficiency whose

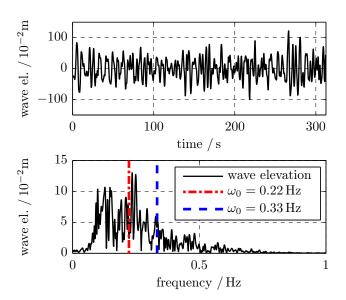


Fig. 2. Wave recorded at Galway Bay in the time and frequency domain.

value $(\eta \text{ or } 1/\eta)$ depends on whether energy is taken from or fed into the net.

$$P_i = \begin{cases} -\eta u \dot{q} & \text{if } u \dot{q} \ge 0 \\ -\frac{1}{\eta} u \dot{q} & \text{if } u \dot{q} < 0 \end{cases}, 0 \le \eta \le 1$$
 (3)

In essence, this formulation of the instataneous power considers the important power conversion losses in both directions, from mechanical to electrical power and vice versa. This makes power taken from the net more expensive from a control point of view.

2.2 Wave Force

A wave recorded by the Irish Marine Institute (wave rider buoy data from Galway Bay) is used to represent an irregular sea state. The wave is sampled at a frequency of $2.56\,\mathrm{Hz}$. An excerpt of the signal and its spectrum are depicted in Figure 2. The wave force w is considered to be directly proportional to the wave elevation.

3. CONTROL OF THE WEC

This section states the control objective and presents different control strategies. Among the considered strategies are a PI velocity control, force threshold unlatching and two latching control schemes based on a short term wave prediction.

3.1 Control Objective

The control objective is to maximise the energy capture. It is pointed out that mean power which is taken from the system (fed to the net), has a negative sign and thus, the control objective corresponds to the minimisation of the mean power. The mean power P_m is easily calculated as the normed integral over the instantaneous power P_i (3)

$$P_m = \frac{1}{T} \int_{t=0}^{T} P_i \mathrm{d}t. \tag{4}$$

 $^{^{\}rm 1}\,$ The instantaneous power output can be positive and negative, i. e. power can be generated and consumed.

The considered reference control is a PI feedback of the PTO velocity 2 .

$$u = -k_v \dot{q} - k_p q. \tag{5}$$

Due to the simplicity of the control law, a brute force grid-based search method can be applied to find the gains yielding the optimal mean power output achievable with (5). The PI velocity feedback leads to reactive power flows which are more or less significant depending on the chosen gains. The ratio of peak to average power reaches 31 for the optimal gains in the case of perfect PTO efficiency ($\eta=1$). For PTO efficiencies less than 1, high reactive power flows severly decrease the mean power output s.t. the optimal PI gains depend drastically on η . The main advantage of the PI velocity control is that it does not need measurements of the wave force.

3.3 Latching Control

In a latching control strategy, the moving parts of the wave energy converter are successively latched and unlatched. This way, the system is brought in phase (and thus in resonance) with the sea. The approach allows to achieve high velocities which in turn allow to take off high amounts of energy.

If a latching control is applied to the system (1), the closed loop is a switching system with two phases.

(1) The unlatched system with the equations of motion (1) and the PTO force control law

$$u = -k_{v,l}\dot{q}. (6)$$

(2) The latched system with $\ddot{q}=0$ and $\dot{q}=0$ (no movement).

The system can change from phase 1 to phase 2 only if $\dot{q}=0$. This ensures that no energy is consumed for braking the device. Once at rest, the device can be unlatched at any time.

The biggest benefit of latching control is that it is passive, i.e. that it does not need to draw energy from the net $(k_{v,l})$ is negative s.t. $-u\dot{q}$ is negative which corresponds to an energy flow to the net). Active controls, i.e. controls that allow for reversible energy flows, need PTOs of higher complexity which are more expensive.

The challenge in latching control consists of finding the precise times at which to unlatch the body - especially in a realistic irregular sea state. But before the strategies to determine the latching timing are discussed, a choice for the PTO force control law (6) is made.

Choice of the PTO Force Control Law The gain $k_{v,l}$ in the PTO force control law (6) is often considered as given (see e. g. Babarit et al. (2004); Babarit and Clément (2006)) or, for simpler schemes, found by gridding over all possible values (see e. g. Falcão (2008)). In order to systematically determine a good practise for the choise of $k_{v,l}$, the optimal latching control problem in monochromatic waves

$$w = A_w \cos(\omega t + \varphi) \tag{7}$$

is considered in this paper. In an irregular sea with the dominant frequency ω_d , the gain which is optimal for a monochromatic wave with the frequency ω_d is implemented.

The optimal latching control in monochromatic waves is determined using the knowlege that the system approaches a periodic trajectory on which the system switches between the two phases 'latched' and 'unlatched'. In the highest and lowest point of the periodic trajectory, when the velocity is zero, the system is latched. The phase φ of the wave when the system is to be unlatched can be determined based on the following considerations, see e.g. Babarit and Clément (2006); Babarit et al. (2004). The initial state of the system in the moment of unlatching is the position $q_0 = \zeta_0$ and velocity $\dot{q}_0 = 0$. From the periodic nature of the final trajectory, it can be deduced that after half a period of the controlled motion, the system is latched again in the position $q_1 = -\zeta_0$ when its velocity is $\dot{q}_1 = 0$. Instead of directly maximising the mean power output, the problem is usually simplified to finding the φ which leads to the maximum amplitude ζ_0 . In the following treatise, $\boldsymbol{x} = \left[q \ \dot{q} \right]^T.$

With the undamped eigenfrequency

$$\mu = \sqrt{\omega_0^2 - \zeta^2 \omega_0^2} \tag{8}$$

and a, b (which depend on the initial values), the solution of the wave energy generator equations of motion (1) to a monochromatic wave (7) is given by

$$q(t) = (a\cos(\mu t) + b\sin(\mu t)) e^{-\zeta\omega_0 t} + |H(\omega)| A_w \cos(\varphi + \omega t + \angle H(\omega)).$$
 (9)

Using this explicit solution of the wave energy converter's equations of motion (9) (without loss of generality, the initial time t_0 is set to 0), the problem which is to be solved in order to find the optimal ϕ can be formulated as

$$\max_{\varphi} \zeta_0 \text{ s. t.} \tag{10}$$

$$x(t_0) = [\zeta_0 \ 0]^T, x(t_1) = [-\zeta_0 \ 0]^T \text{ and } (9)$$
 (11)

There are 5 unknowns φ , a, b, t_1 and ζ_0 which can be solved for using the 4 boundary conditions (11) and the optimum condition max ζ_0 . Because the equations are highly nonlinear, a semi-numerical solution is called for e.g.

- (1) eliminate a and b using $\boldsymbol{x}(t_0) = \begin{bmatrix} \zeta_0 & 0 \end{bmatrix}^T$,
- (2) using a and b from step 1, solve $\mathbf{x}(0) = -\mathbf{x}(t_1)$ for ζ_0 (now a function of t_1 and φ),
- (3) find the maximum ζ_0 over a grid of t_1 and φ .

It is not surprising that, for excitation frequencies slower than the undamped eigenfrequency μ of the device, the optimal t_1 equals half a natural period of the undamped eigenfrequency

$$T = 2\pi/\mu. \tag{12}$$

The control approach brings the system in resonance with the wave force. The resulting velocity of the wave energy converter is in phase with the excitation force. Similar calculations are also possible for systems of higher complexity, e.g. for systems with a dynamic radiation force/added mass, see Babarit and Clément (2006).

 $^{^2}$ This corresponds to a full state feedback for the simple model considered in this paper

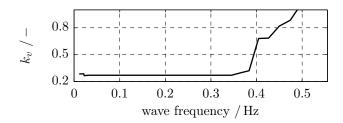


Fig. 3. Results of the line search for $k_{v,l}$ (case $\omega_0 = 0.22\,\mathrm{Hz}$).

Using the above results, the gain $k_{v,l}$ which leads to optimal energy extraction can be found for each wave frequency by performing a line search consisting of two steps.

- (1) The damping of the system is modified to account for the proportional gain $k_{v,l}$ s.t. $\tilde{d} = d + k_{v,l}$. Starting from $k_{v,l} = 0.05\zeta\omega_0$, $k_{v,l}$ is increased and the optimisation problem (11) is solved for each value of $k_{v,l}$. Based on the obtained latching timings, the mean power output with the individual $k_{v,l}$ over t_1 is calculated. This is repeated until the obtained mean power decreases for the first time in the k^{th} step.
- (2) A golden section search is started between the $(k-2)^{\text{th}}$ and the k^{th} step in order to find the $k_{v,l}$ yielding the highest power output.

The results of this approach for the considered wave energy converter are depicted in Figure 3 for the case $\omega_0 = 0.22\,\mathrm{Hz}$.

A gain $k_{v,l}$ obtained by the procedure described above leads to good results in irregular waves as shown in the following section. From the characteristic of the optimal $k_{v,l}$ over the frequency, given in Figure 3, it is already clear that $k_{v,l}$ does not change significantly over a wide band of relevant frequencies around the eigenfrequency of the device.

Threshold Unlatching This simple but effective scheme to determine the latching timing in an irregular sea was proposed e.g. in Falcão (2008). The device is unlatched as soon as the incident wave force exceeds a certain threshold. Accordingly, this strategy merely needs a measurement of the incident wave force and no prediction. The choice of the force threshold depends on the sea state. Again, the control law can easily be optimized by using a grid based search (the threshold and the gain $k_{v,l}$ are the only parameters).

At the example of the threshold unlatching control it is shown that the choice of the gain $k_{v,l}$, which is proposed in Section 3.3.1, leads to good results in irregular waves. Simulations are performed with the optimal $k_{v,l}$, obtained from the grid based search, and the $k_{v,l}$ which results from the procedure given in Section 3.3.1. The two resulting energy outputs are almost equal: the difference is below 0.5%.

Model Based Predictive Latching The model based predictive latching is proposed in Babarit et al. (2004). Each time the system is latched after reaching zero velocity, the prediction horizon is gridded leading to a sequence of possible unlatching times t_i . For each t_i , the energy generated between t_i and the next zero-crossing of the

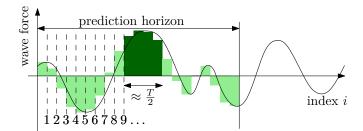


Fig. 4. The principle of mean wave force predictive latching.

velocity is calculated by simulating the system response. In the end, the system is unlatched at the t_i leading to the highest energy output.

It is pointed out explicitly, that even though the latching timing is selected optimally with respect to the limited prediction horizon, it is not globally optimal. Because of the discrete nature of the control law, a decision at time t_a may have undesired effects for a later time t_b (which is not part of the prediction horizon). Obvious disadvantages of the scheme are its dependence on the full model of the WEC and the fact that a full state feedback is needed to initialize the simulations used to determine the energy output predictions.

Mean Wave Force Predictive Latching An alternative approach, newly proposed in this paper, is to unlatch the system during a period when the predicted mean wave force has the correct sign and a high absolute value. This approach to calculate the latching timing with a prediction of the wave force is sketched in Figure 4.

From Section 3.3.1, it is known that the unlatched motion should roughly last for about half of the period T (12) of the wave energy converter. For models of higher complexity, this corresponds to half a period of the undamped frequency of the system's dominating mode. The predicted wave force is sampled (sample time T_s) s.t. an integer multiple of the sample time corresponds to $T/2 = NT_s$. In the example of Figure 4, N=4. Starting from each sample of the prediction horizon, windows of length $T/2=NT_s$ are integrated in order to determine their corresponding mean wave force. The integration is performed e. g. using a simple Euler rule.

$$I_i = \sum_{k=i}^{N+i-1} T_s w_{pred}(kT_s)$$
 (13)

Based on the information about the predicted mean wave force in all the windows I_i , the timing of the unlatching is determined. The window with the maximum mean force is the window with the maximum integral, denoted I_{max} (with index i_{max}). Should the device be in its lower latched position, it is a good practise to unlatch it at $t = (i_{max} - 1)T_s$ (the initial time of the window with the maximum mean up-force). This is the scenario depicted in Figure 4. The marked samples represent the period with the maximum mean up-force, i. e. the time during which the device should be unlatched. Respectively, if the device is in its upper latched position, the window with the minimum integral is chosen to time the unlatching. The necessary length of the prediction horizon mainly depends on the characteristics of the incoming wave. A prediction horizon

of 1.3 times the dominating period of the wave already yields good results.

This scheme is similar to other schemes which try to synchronize the maximum wave force with the maximum device velocity as e.g. Eidsmoen (1998). Because of the averageing, the proposed approach is more robust with respect to noisy, imperfect wave force predictions.

4. SHORT-TERM WAVE PREDICTION

The approach most commonly used in the literature (Fusco and Ringwood (2010b,a); Schoen et al. (2011)) is the online identification of an AR model of the order n_{AR} :

$$y_i = \sum_{k=1}^{n_{AR}} a_k y_{i-k}.$$
 (14)

The parameter vector

$$\boldsymbol{a} = \begin{bmatrix} a_1 \ a_2 \ \dots \ a_{n_{AR}} \end{bmatrix}^T \tag{15}$$

characterises the AR model.

An equivalent representation of the AR model (14) is found with

$$\begin{bmatrix} y_i \\ y_{i-1} \\ \vdots \\ y_{i-n_{AR}+1} \end{bmatrix} = \begin{bmatrix} a_1 & a_2 & \dots & a_{n_{AR}-1} & a_{n_{AR}} \\ 1 & 0 & \dots & 0 & 0 \\ 0 & 1 & \dots & 0 & 0 \\ 0 & 0 & \ddots & 0 & 0 \\ 0 & 0 & \dots & 1 & 0 \end{bmatrix} \begin{bmatrix} y_{i-1} \\ y_{i-2} \\ \vdots \\ y_{i-n_{AR}} \end{bmatrix},$$

 $\boldsymbol{x}_i = \boldsymbol{A}_{ar}(\boldsymbol{a})\boldsymbol{x}_{i-1},\tag{17}$

(16)

$$y_i = \underbrace{\begin{bmatrix} 1 & 0 & \dots & 0 \end{bmatrix}}_{\boldsymbol{C_{ar}}} \boldsymbol{A_{ar}}(\boldsymbol{a}) \boldsymbol{x_{i-1}}. \tag{18}$$

Once a suitable model of the type (16) is identified for the wave signal, it may be extrapolated as

$$y_{i+l-1|i-1}(\boldsymbol{a}) = \underbrace{\begin{bmatrix} 1 & 0 & \dots & 0 \end{bmatrix}}_{C_{ar}} \boldsymbol{A}_{ar}(\boldsymbol{a})^{l} \boldsymbol{x}_{i-1}.$$
 (19)

The notation $y_{i+l-1|i-1}(\boldsymbol{a})$ specifies that the *l*-step-ahead prediction of y is calculated based on measurements up to the step i-1 and that this prediction depends on the choice of \boldsymbol{a} .

The AR model identification, i.e. the identification of the parameter vector \boldsymbol{a} , is performed with the objective to minimise a multi-step-prediction over multiple (past) horizons as proposed in Fusco and Ringwood (2010a). With a finite set of samples \mathcal{T} up to the current one, such a criterion can be formulated as

$$J_{lrp}(\boldsymbol{a}) = \sum_{k \in \mathcal{T}} \sum_{j=1}^{l} (y_k - y_{k|k-j}(\boldsymbol{a}))^2.$$
 (20)

Because of (19), this criterion is a nonlinear least squares problem. No constraints on the decision variables a are enforced s.t. the optimisation problem simply reads

$$\min_{\boldsymbol{a}} J_{lrp}(\boldsymbol{a}).$$
(21)

Once an AR model is identified, it remains valid for several minutes. This allows to perform the identification in a

batch job using past data, even in real-time applications. In this paper, a Levenberg-Marquardt nonlinear least squares algorithm is applied. It is noted that in order to predict the wave force with the methods presented in this section, the wave force must be a measurable external signal of the system.

Several options are important to obtain good results for the prediction:

- sample time of the AR model Δt_{AR} ,
- pre-filtering of the wave signal,
- order of the AR model n_{AR} ,
- wave prediction horizon (in samples) $n_{w,pred}$,
- number of horizons considered in the identification n_{hor} .

These options are discussed in the following paragraphs.

Sample Time of the AR Model — The sample time of the AR model has a huge impact on the prediction quality due to its filtering properties and its impact on the effective prediction horizon $T_{w,pred} = \Delta t_{AR} n_{w,pred}$. In this paper, it is chosen depending on the dominant wave frequency ³ ω_d s.t.

$$\Delta t_{AR} = \frac{2\pi}{13\omega_d}. (22)$$

Pre-filtering of the Wave Signal A pre-filtering of the wave signal can greatly increase the prediction performance, see e.g. Fusco and Ringwood (2010a). Non-causal filtering techniques are often used in order to avoid a phase lag of the estimated signal, see Fischer et al. (2012). The issues concerning the trade off between non-causality (which can possibly be compensated by a longer prediction horizon) and phase lag remain an open problem. In this paper, the filter was chosen following the recommendations of Fusco and Ringwood (2010a).

Order of the AR Model The order of the AR model corresponds to twice the number of harmonics that are modelled. There is a trade-off between model complexity (which increases the difficulty to solve the identification problem) and prediction performance. In this work, n_{AR} is set to 32.

Prediction Horizon Like the order of the AR model, this parameter represents a trade-off between the complexity of the identification problem and the prediction performance. On the one hand, the higher $n_{w,pred}$, the 'more nonlinear' the identification problem due to (19). On the other hand, a low $n_{w,pred}$ often results in an unstable AR model. This is why a relatively high prediction horizon of $n_{w,pred} = 50$ is chosen. Of that long horizon, only a few first steps approximate the future wave well. The prediction horizon considered in the identification is thus much higher than the prediction horizon needed for the latching control strategies.

Number of Horizons Considered The number of horizons which is considered smooths the results and thus increases their long term validity. The more horizons are considered, the higher the computational effort for the evaluation of the objective function of the identification (20). In

³ The frequency with the highest power

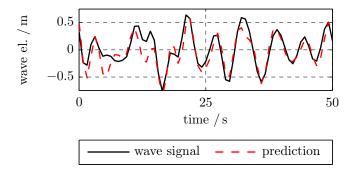


Fig. 5. 6 s-ahead wave prediction based on the identified AR model.

practise, every $25^{\rm th}$ value over a horizon of the last $300\,\rm s$ is considered in the set $\mathcal{T}.$

In the considered application, the first 500 s of wave data are used for the identification of the AR model which is then used to predict the wave. The resulting prediction quality for a 6 s-ahead prediction after 800 s of the wave signal (training window and prediction window are well separated) is depicted in Figure 5.

The poles of the optimised AR model are predominantly on the unit circle (0-damping line) representing the harmonic nature of the identified signal.

5. SIMULATION RESULTS

A simulation study is performed using the two configurations of the generic WEC which differ in their resonance frequencies (0.22 Hz and 0.33 Hz). The energy produced by all control approaches considered in this report is calculated on a predefined interval of the wave recorded at Galway Bay (between 750 s and 1000 s). This allows to perform the identification of the AR model for the wave prediction based on past data - an important real-time constraint.

Some simulation results for the case $\omega_0 = 0.22\,\mathrm{Hz}$ are given in the form of system trajectories. Figure 6 captures the product of control and velocity (instantaneous power) of the PI velocity controls for different values for the PTO efficiency. The lower the efficiency of the PTO, the less power is taken from the net. Obviously, the PI velocity control scales badly with a lower PTO efficiency since both negative effects show their impact: power taken from the net becomes more expensive and the produced power is reduced. This is a big advantage of the latching controls which do not need to draw power from the net such that they are only effected by the lower mechanical to electrical power conversion efficiency. This also means that the same latching control law is applicable to different efficiency coefficients η - in contrast to the PI velocity control which strongly depends on η . The Figures 7 and 8 show the trajectories of the device velocity together with the incident wave force for the PI velocity control and the threshold unlatching control. The trajectory of wave force and device velocity for the two predictive latching schemes are given in Figure 9. Even though the mean force predictive control is much simpler, it leads to the same

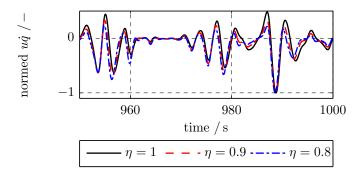


Fig. 6. The product of control and velocity (instantaneous power) of the PI velocity controls for different values for the PTO efficiency.

device motion and thus to the same average power output (in fact it is even slightly higher).

The resulting mean power outputs are captured by Table 1. The power output is always normalized row-wise (for each efficiency coefficient η) with respect to the power output of the PI velocity control. Normalized mean power outputs greater than 1 indicate that the corresponding control does better than the PI velocity control. It is quite interesting to note the different results for the two different WEC.

The only scenario in which the PI velocity control performs better than the latching controls is the case in which the eigenfrequency of the WEC is much higher than the dominant wave frequency ($\omega_0=0.33$) with perfect PTO efficiency. By using a lot of reactive power, the PI velocity control can bring the device in resonance with the wave and extract a high amount of energy. As soon as the PTO efficiency drops lower than 1 however, the passive latching control schemes outperform the PI velocity control.

Both predictive latching schemes yield almost the same power output. In the case of the slower WEC ($\omega_0 = 0.22$), the mean force latching control performs slightly better than the model based latching. On first thought, this seems astonishing. However, the reader is reminded that in the end both schemes are globally suboptimal due to the limited predicion horizon. Clearly, the imperfect prediction leads to higher performance losses in the case of the faster WEC ($\omega_0 = 0.33$). The reason for this is that the latching timing is determined based on shorter windows (proportional to the period of the systems dominant eigenfrequency) of the prediction horizons s.t. local errors have a higher impact. The threshold unlatching even outperforms the predictive latching schemes using the AR model predictions in the case of the faster WEC. The performance gap between threshold unlatching and predictive unlatching is smaller for the faster WEC because the WEC eigenfrequency is further away from the dominant frequencies in the wave spectrum which allows to use higher force thresholds.

6. SUMMARY

Different predictive and non-predictive latching control schemes were benchmarked against a PI velocity control

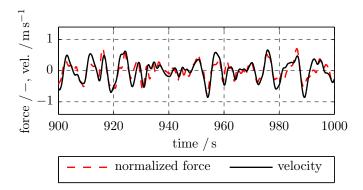


Fig. 7. The incident wave force and the resulting velocity of the PTO: PI velocity control.

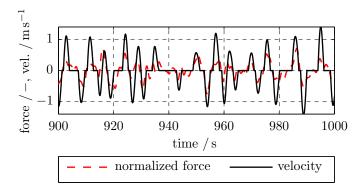


Fig. 8. The incident wave force and the resulting velocity of the PTO: threshold unlatching.

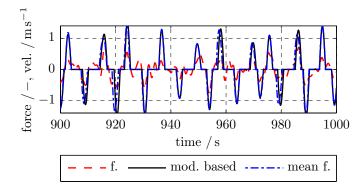


Fig. 9. The incident wave force (f.) and the resulting velocity of the PTO: model based predictive latching (mod. based) and mean wave force predictive latching (mean f.).

in an irregular sea. Considering imperfect mechanical to electrical and electrical to mechanical power conversion shows the benefit of the latching controls with respect to the PI velocity feedback. Depending on the ratio between system resonance frequency and dominant wave frequency, the predictive latching schemes are more or less sensitive to imperfect wave force predictions. For fast WEC, whose controls are more sensitive to imperfect wave predictions, the considered non-predictive latching scheme can show off its advantages.

7. ACKNOWLEGEMENTS

The authors would like to thank the Irish Marine Institute for providing the wave elevation measurements used in this study.

REFERENCES

A Babarit and AH Clément. Optimal latching control of a wave energy device in regular and irregular waves. Applied Ocean Research, 28(2):77–91, 2006.

Auréelien Babarit, Gaielle Duclos, and AH Clemént. Benefit of latching control for a heaving wave energy device in random sea. In 13th Int Offshore and Polar Engineering Conference, volume 1, pages 341–348, 2003.

Aurélien Babarit, Gaelle Duclos, and Alain H Clément. Comparison of latching control strategies for a heaving wave energy device in random sea. *Applied Ocean Research*, 26(5):227–238, 2004.

K. Budal, J. Falnes, L.C. Iversen, P.M. Lillebekken, G. Oltedal, T. Hals, and T. Onshus. The norwegian wave-power buoy project. In *The Second International* Symposium on Wave Energy Utilization, 1982.

H. Eidsmoen. Tight-moored amplitude-limited heavingbuoy wave-energy converter with phase control. Applied Ocean Research. 20(3):157 – 161, 1998. ISSN 0141-1187.

A. F. O. Falcão. Phase control through load control of oscillating-body wave energy converters with hydraulic pto system. *Ocean Engineering*, 35(3):358–366, 2008.

B. Fischer, P. Kracht, and S. Perez-Becker. Online-algorithm using adaptive filters for short-term wave prediction and ist implementation. In *Proceedings of the ICOE 2012*, 2012.

Francesco Fusco and John V Ringwood. Short-term wave forecasting for real-time control of wave energy converters. Sustainable Energy, IEEE Transactions on, 1(2):99–106, 2010a.

Francesco Fusco and John V Ringwood. Short-term wave forecasting with AR models in real-time optimal control of wave energy converters. In *Industrial Electronics* (ISIE), 2010 IEEE International Symposium on, pages 2475–2480. IEEE, 2010b.

Rico Hjerm Hansen and Morten M. Kramer. *Modelling* and Control of the Wavestar Prototype. University of Southampton, 2011.

M.P. Schoen, J. Hals, and T. Moan. Wave prediction and robust control of heaving wave energy devices for irregular waves. *Energy Conversion*, *IEEE Transactions* on, 26(2):627–638, 2011. ISSN 0885-8969.

Table 1. Performance Comparison.

WEC model ω_0	PTO eff. η	PI-velocity	thresh. latch.	model based latch.	model based latch. AR pred.	mean force latch.	mean force latch. AR pred.
0.22	1	1	1.06	1.20	1.11	1.24	1.17
	0.9	1	1.15	1.31	1.21	1.35	1.28
	0.8	1	1.23	1.40	1.29	1.44	1.36
0.33	1	1	0.86	0.89	0.76	0.89	0.76
	0.9	1	1.12	1.16	1.00	1.17	1.00
	0.8	1	1.34	1.39	1.19	1.39	1.19